IDENTIFIABILITY ANALYSIS OF SENSOR ARRAYS WITH SENSORS OFF HALF-WAVELENGTH GRID

Md. Waqeeb T. S. Chowdhury[†], *Yimin D. Zhang*[†], *Wei Liu*[‡], *and Maria S. Greco*[§]

[†] Department of Electrical and Computer Engineering, Temple University, USA
[‡] School of Electronic Engineering and Computer Science, Queen Mary University of London, UK
[§] Department of Ingegneria dell'Informazione, University of Pisa, Italy

ABSTRACT

In this paper, we analyze the effect of sensor placement to the achievable number of degrees-of-freedom (DOFs) when the sensors deviate from a half-wavelength grid. More specifically, we consider two variations of a uniform linear array (ULA), namely, when one or more sensors are shifted from half-wavelength grid positions and when the inter-element spacing of the ULA is smaller than a half-wavelength. The numerical rank and the rank-revealing QR factorization of the array data covariance matrix are examined and the number of DOFs of the array is studied in terms of the rank of the array data covariance matrix. A threshold based on the rank-revealing QR factorization is proposed to separate the eigenvalues respectively corresponding to the signal and noise subspaces, and thus the numerical rank of the array data covariance matrix is estimated. Simulation results are provided to justify the findings and provide insights on sensor placements to preserve the array DOFs.

***Index Terms*—** Direction-of-arrival estimation, degrees-of-freedom, non-integer array, rank analysis, QR factorization.

1. INTRODUCTION

Direction-of-arrival (DOA) estimation of signals using an array of sensors is one of the most widely studied problems in the field of array signal processing [1, 2]. Due to the Nyquist sampling theorem, the most commonly used sensor array is the uniform linear array (ULA), which consists of sensors that are linearly and uniformly placed along the integer multiples of half the signal wavelength. It is well known that ULAs equipped with N omnidirectional sensors offer $N-1$ degrees-of-freedom (DOFs). A number of sparse linear array structures [3–10] have been studied over the past decade that provide additional DOFs compared to a ULA by leveraging the correlation lags provided by the difference coarray [11, 12]. Increased array DOFs and improved performance are further achieved by exploiting wideband and multi-frequency signals [13–16] as well as sensor motion [17, 18].

The majority of linear arrays being considered in the literature, regardless whether they are uniform or sparse, is limited to arrays where the sensors are placed along the half-wavelength grid. On the other hand, the effect of sensor position perturbation to the array sensing capability and performance has not been adequately investigated in the literature. In this paper, we consider a simple problem by investigating how the number of achievable DOFs for a linear array varies when the sensors are placed off the half-wavelength grid. We refer to arrays with all sensors placed on the half-wavelength grid as integer arrays, whereas any arrays that violate this condition as non-integer arrays.

There are studies on the optimized design and application of non-integer linear arrays for interference suppression [19] and DOA estimation [20, 21]. In [19], a technique was developed to suppress interference signals by optimizing the sensor positions, rendering non-integer arrays as the optimization solution. A Fourier domain root-MUSIC method was proposed in [20] for DOA estimation using arbitrary two-dimensional arrays. The non-Toeplitz structure of the covariance matrix of non-integer arrays was studied in [21] and an interpolation technique was proposed to detect more uncorrelated signals than sensors in the coarray domain. However, the number of DOFs is not considered in these works.

Recent advances in rational array design [22, 23] have sparked a wave of interest in non-integer arrays. In [22, 23], the performance of rational sparse arrays and the conditions for unique identifiability and unambiguous detection of signals were analyzed. An irregular Vandermonde decomposition was introduced in [24] that extends the conventional Vandermonde decomposition to a broader range of matrices. The concept of rational sparse arrays was extended to the design of multi-frequency coprime rational arrays exploiting reduced frequency separation in [25]. It is pointed out that, while the utilization of rational frequencies offers great flexibility in the multi-frequency sparse array design [14, 16] and the resulting virtual rational coprime array, it becomes more important to take the spatial correlation or sidelobe issues into account. Bearing this in mind, the condition for unique identifiability and unambiguous source detection was examined in [26].

With increased interest in such non-integer arrays, it is important to examine the potential number of DOFs that can be achieved with such arrays. In this paper, we study how the achievable number of DOFs of an N-element ULA would vary when it violates the integer array conditions. We focus on two cases, namely, when one sensor is shifted from its original half-wavelength grid position and when the inter-element spacing of the entire ULA is compressed to a value that is smaller than a half-wavelength. We analyze how the smallest signal subspace (SS) eigenvalue varies in these two scenarios. A QR factorization-based threshold level for the separation of signal and noise subspaces is defined, and the numerical rank of the covariance matrix is analyzed by observing the smallest SS eigenvalue.

Notations: We use lower-case (upper-case) bold characters to denote vectors (matrices). In particular, $\mathbf{I}_N$ denotes the $N \times N$ identity matrix and $\mathbf{0}$ stands for a vector or matrix of all zeros with a proper dimension. $(\cdot)^*$, $(\cdot)^{\mathrm{T}}$, $(\cdot)^{\mathrm{H}}$ and $\mathbb{E}[\cdot]$ respectively represent the complex conjugate, transpose, Hermitian, and statistical expectation operations. $\mathrm{diag}(\cdot)$ forms a diagonal matrix and $\mathrm{Tr}(\cdot)$ rep-

The work of M. W. T. S. Chowdhury and Y. D. Zhang was supported in part by National Science Foundation (NSF) under Grant No. ECCS-2236023.

resents the trace operator. In addition, $\mathbf{x}_i$ denotes the ith element of vector $\mathbf{x}$ and $\jmath = \sqrt{-1}$ stands for the unit imaginary number. The spectral norm of matrix $\mathbf{B}$ is its largest singular value, given as $||\mathbf{B}||_2 = \sqrt{\lambda_{\max}(\mathbf{B}^{\mathrm{H}}\mathbf{B})}$, where $\lambda_{\max}(\cdot)$ returns the largest eigenvalue. Finally, $\mathbb{C}^{M\times N}$ denotes the $M \times N$ complex space.

2. SIGNAL MODEL

Consider a ULA with N omnidirectional sensors and $L < N$ far-field uncorrelated narrowband signals impinging on the array from distinct angles $\boldsymbol{\theta} = [\theta_1, \cdots, \theta_L]^{\mathrm{T}}$. The baseband signal vector received at the array is expressed as

$$\mathbf{x}(t) = \sum_{l=1}^{L} \mathbf{a}(\theta_l) s_l(t) + \mathbf{n}(t) = \mathbf{A}\mathbf{s}(t) + \mathbf{n}(t), \tag{1}$$

where $\mathbf{a}(\theta) = [e^{-\jmath p_1 \pi \sin(\theta)}, e^{-\jmath p_2 \pi \sin(\theta)}, \cdots, e^{-\jmath p_N \pi \sin(\theta)}]^{\mathrm{T}}$ is the steering vector of the array for signal impinging from angle θ, p_n denotes the position of the nth sensor scaled to the half-wavelength unit, $s_l(t)$ denotes the signal waveform impinging from direction θ_l, $\mathbf{s}(t) = [s_1(t), \cdots, s_L(t)]^{\mathrm{T}}$, and $\mathbf{n}(t)$ represents the zero-mean additive circularly complex white Gaussian noise vector observed at the array with covariance matrix $\sigma_{\mathrm{n}}^2\mathbf{I}_N$. In addition, $\mathbf{A} = [\mathbf{a}(\theta_1), \mathbf{a}(\theta_2), \cdots, \mathbf{a}(\theta_L)] \in \mathbb{C}^{N\times L}$ denotes the ULA manifold matrix. The covariance matrix of the received data vector is obtained as

$$\mathbf{R}_x = \mathbb{E}\left[\mathbf{x}(t)\mathbf{x}^{\mathrm{H}}(t)\right] = \mathbf{A}\mathbf{R}_s\mathbf{A}^{\mathrm{H}} + \sigma_n^2\mathbf{I}_N, \tag{2}$$

where $\mathbf{R}_s = \mathbb{E}\left[\mathbf{s}(t)\mathbf{s}^{\mathrm{H}}(t)\right] = \mathrm{diag}\left(\left[\sigma_1^2, \sigma_2^2, \cdots, \sigma_L^2\right]\right)$ is the source covariance matrix. In practice, the covariance matrix is estimated from K snapshots of the available received data as

$$\hat{\mathbf{R}}_x = \frac{1}{K}\sum_{t=1}^{K} \mathbf{x}(t)\mathbf{x}^{\mathrm{H}}(t). \tag{3}$$

Performing eigen-decomposition on the received data covariance matrix yields

$$\mathbf{R}_x = \mathbf{U}\mathbf{\Lambda}\mathbf{U}^{\mathrm{H}} = \sum_{p=1}^{L} \lambda_p \mathbf{u}_p\mathbf{u}_p^{\mathrm{H}} + \sum_{q=L+1}^{N} \lambda_q \mathbf{u}_q\mathbf{u}_q^{\mathrm{H}}, \tag{4}$$

where $\mathbf{U} = [\mathbf{u}_1, \mathbf{u}_2, \cdots, \mathbf{u}_N]$ contains all eigenvectors, and $\mathbf{\Lambda} = \mathrm{diag}([\lambda_1, \lambda_2, \cdots, \lambda_N])$ denotes a diagonal matrix containing the corresponding eigenvalues.

Ideally, when the eigenvalues are sorted in a descending order, the smallest $N - L$ eigenvalues corresponding to the noise subspace (NS) are equal to the noise power σ_n^2 so that $\lambda_1 \geq \lambda_2 \geq \cdots \geq \lambda_L > \lambda_{L+1} = \cdots = \lambda_N = \sigma_n^2$. In practice, however, as the estimated covariance matrix $\hat{\mathbf{R}}_x$ is computed based on a limited number of snapshots, the eigenvalues corresponding to the NS are generally not equal to the noise power. In this case, the estimated eigenvalues are related as $\hat{\lambda}_1 \geq \hat{\lambda}_2 \geq \cdots \geq \hat{\lambda}_L > \hat{\lambda}_{L+1} \geq \cdots \geq \hat{\lambda}_N$. As indicated in [27], in such a non-ideal scenario, when perfect statistics of the received data are not available, a challenging task is to determine a proper threshold $\hat{\lambda}_{\mathrm{thr}}$ between the smallest eigenvalue $\hat{\lambda}_L$ of the SS and the largest eigenvalue of the NS $\hat{\lambda}_{L+1}$ such that $\hat{\lambda}_L > \hat{\lambda}_{\mathrm{thr}} > \hat{\lambda}_{L+1}$.

3. NUMERICAL RANK AND RANK-REVEALING QR FACTORIZATION OF THE COVARIANCE MATRIX

3.1. Numerical Rank of the Covariance Matrix

For an arbitrary matrix $\mathbf{D} \in \mathbb{C}^{N\times N}$, its numerical rank $r \leq N$ with respect to a small positive tolerance $\mathcal{O}(\epsilon)$ is defined as [28]

$$r = \min\{\mathrm{rank}(\mathbf{B}) : \mathbf{B} \in \mathbb{C}^{N\times N},\ ||\mathbf{D} - \mathbf{B}||_2 \leq \mathcal{O}(\epsilon)\}. \tag{5}$$

The numerical rank r of $\mathbf{D}$ is equal to the number of columns that are linearly independent for any perturbation of $\mathbf{D}$ with a norm at most of the tolerance $\mathcal{O}(\epsilon)$.

It is noted that, for the underlying array covariance matrix considered here, the smallest estimated NS eigenvalues are not $\mathcal{O}(\epsilon)$, rather they are $\sigma_n^2 + \mathcal{O}(\epsilon)$ such that $\mathcal{O}(\epsilon) \to 0$ as $K \to \infty$. In this case, the term $\mathcal{O}(\epsilon)$ denotes the tolerance of the estimated NS eigenvalues from its true value of σ_n^2 when the number of available snapshots is finite. Therefore, the numerical rank of the array covariance matrix can be alternatively defined as follows:

Definition: For a given $\mathcal{O}(\epsilon) > 0$, the numerical rank of the array covariance matrix $\hat{\mathbf{R}}_x \in \mathbb{C}^{N\times N}$ is the smallest integer $r \leq N$ such that $\lambda_r > \sigma_n^2 + \mathcal{O}(\epsilon)$.

3.2. Rank-Revealing QR Factorization

When the distance between two or more sensors is less than half-wavelength, the magnitude of the smallest eigenvalue of the SS will be closer to that of the NS. This makes it more challenging to establish a boundary that separates the SS eigenvalues from the NS ones. Instead of directly examining the eigenvalues, in this paper, we exploit the rank-revealing QR factorization to evaluate the rank of the array covariance matrix.

The threshold for separating the signal and noise subspaces can be analyzed using the QR factorization of the covariance matrix of the array data vector. The concept of numerical rank discussed in [29] along with the rank-revealing properties of QR factorization [30, 31] can be utilized to study the identifiability of the antenna array when one or more sensors are shifted from the integer positions to non-integer ones. In the following, we provide brief review for rank-revealing QR factorization, and identifiability analysis for non-integer arrays is considered in the subsequent section for two scenarios.

It is shown in [29] that, if $\hat{\mathbf{R}}_x$ has a numerical rank of r and there exists a permutation matrix $\mathbf{\Pi} \in \{0, 1\}^{N\times N}$ such that performing QR factorization on $\mathbf{\Pi}\hat{\mathbf{R}}_x$ yields

$$\mathbf{\Pi}\hat{\mathbf{R}}_x = \mathbf{Q}\mathbf{R} = \mathbf{Q}\begin{bmatrix}\mathbf{R}_{11} & \mathbf{R}_{12}\\ \mathbf{0} & \mathbf{R}_{22}\end{bmatrix}, \tag{6}$$

and if

$$\lambda_{\min}(\mathbf{R}_{11}) > ||\mathbf{R}_{22}||_2, \tag{7}$$

where $\mathbf{Q} \in \mathbb{C}^{N\times N}$ is an orthonormal matrix, $\mathbf{R} \in \mathbb{C}^{N\times N}$ is an upper triangular matrix, and $\mathbf{R}_{11} \in \mathbb{C}^{r\times r}$ and $\mathbf{R}_{22} \in \mathbb{C}^{(N-r)\times(N-r)}$, then (6) is said to be a rank-revealing QR factorization of $\hat{\mathbf{R}}_x$.

As $\hat{\mathbf{R}}_x$ is full rank in the presence of noise, there exists a permutation matrix $\mathbf{\Pi}$ such that in (6) the diagonal entries of the upper triangular matrix $\mathbf{R}$ are in a decreasing order. Since the eigenvalues of any upper triangular matrix are the diagonal entries themselves [32], it implies that, for any array covariance matrix $\hat{\mathbf{R}}_x$, condition (7) is satisfied and a rank-revealing QR factorization of $\hat{\mathbf{R}}_x$ exists. Our objective is to determine the number of eigenvalues belonging

to the SS, i.e., L, from r identified by the QR factorization. From the eigenvalue interlacing property [33, 34], it can be easily shown that $\lambda_r(\hat{\mathbf{R}}_x) = \hat{\lambda}_L \geq \lambda_{\min}(\mathbf{R}_{11})$ and $||\mathbf{R}_{22}||_2 \geq \lambda_{r+1}(\hat{\mathbf{R}}_x) = \hat{\lambda}_{L+1}$ always hold. Therefore, we have

$$\hat{\lambda}_L \geq \hat{\lambda}_{\min}(\mathbf{R}_{11}) > ||\mathbf{R}_{22}||_2 \geq \hat{\lambda}_{L+1} \approx \sigma_n^2 + \mathcal{O}(\epsilon). \quad (8)$$

It is observed from (8) that the spectral norm of $\mathbf{R}_{22}$ can be chosen as the suitable threshold value $\hat{\lambda}_{\text{thr}}$ to separate the SS and NS eigenvalues and thus determine the numerical rank of $\hat{\mathbf{R}}_x$.

4. EFFECTS OF NON-INTEGER SENSOR LOCATIONS ON SMALLEST SS EIGENVALUES

In this section, we investigate how the eigenvalues of the covariance matrix of the array data vector are affected when the position of the array sensors deviates from the half-wavelength grid, given a fixed number of sources L. Two cases are considered. In the former, for an N-element ULA with sensors placed along the half-wavelength grid, we shift one of its sensors, originally located at an integer location, p_l, to a non-integer position and varies between p_l-1 and p_l+1. For the latter case, the sensors in the N-element ULA remain uniformly spaced but their inter-element spacing is compressed by a factor $\alpha \leq 1$. In both cases, we observe how the smallest SS eigenvalue as well as the numerical rank of the covariance matrix vary.

We express (4) in a matrix format as

$$\mathbf{R}_x = \mathbf{U}_s\mathbf{\Lambda}_s\mathbf{U}_s^{\text{H}} + \mathbf{U}_n\mathbf{\Lambda}_n\mathbf{U}_n^{\text{H}}, \quad (9)$$

where $\mathbf{U}_s = [\mathbf{u}_1, \cdots, \mathbf{u}_L]$, $\mathbf{U}_n = [\mathbf{u}_{L+1}, \cdots, \mathbf{u}_N]$, $\mathbf{\Lambda}_s = \text{diag}([\lambda_1, \cdots, \lambda_L])$, and $\mathbf{\Lambda}_n = \text{diag}([\lambda_{L+1}, \cdots, \lambda_N])$. Define $\mathbf{\Lambda}_s' = \mathbf{\Lambda}_s - \sigma_n^2\mathbf{I}_L$. Then, (9) can be written as

$$\begin{aligned}\mathbf{R}_x &= \mathbf{U}_s(\mathbf{\Lambda}_s' + \sigma_n^2\mathbf{I}_L)\mathbf{U}_s^{\text{H}} + \mathbf{U}_n\mathbf{\Lambda}_n\mathbf{U}_n^{\text{H}} \\ &= \mathbf{U}_s\mathbf{\Lambda}_s'\mathbf{U}_s^{\text{H}} + \sigma_n^2\mathbf{I}_N.\end{aligned} \quad (10)$$

Comparing (2) and (10), we observe that $\mathbf{A}\mathbf{R}_s\mathbf{A}^{\text{H}} = \mathbf{U}_s\mathbf{\Lambda}_s'\mathbf{U}_s^{\text{H}}$. When considering all the impinging signals to have an equal power, denoted as σ_s^2, we have

$$\mathbf{A}\mathbf{A}^{\text{H}} = \frac{1}{\sigma_s^2}\mathbf{U}_s\mathbf{\Lambda'}_s\mathbf{U}_s^{\text{H}}, \quad (11)$$

which suggests that the eigenvalues of the covariance matrix $\mathbf{R}_x$ and those of the matrix $\mathbf{A}\mathbf{A}^{\text{H}}$ are proportional, and their corresponding eigenvectors are identical.

It is note that, for any N-element array with $L < N$ impinging signals, the sum of the eigenvalues of the covariance matrix of the received array data vector is the summation of the total received signal power and the noise power across all sensors, expressed for the equal-power signal case as

$$\sum_{i=1}^{N}\lambda_i = \text{Tr}(\mathbf{R}_x) = N\sum_{i=1}^{L}\sigma_i^2 + N\sigma_n^2 = \sigma_s^2 NL + N\sigma_n^2. \quad (12)$$

That is, the trace of the covariance matrix will remain constant regardless of the position of the sensors and the spatial location of the signal sources, given a fixed number of sensors and signals.

Because the maximum rank of $\mathbf{A}\mathbf{A}^{\text{H}}$ is L, considering that matrices $\mathbf{A}\mathbf{A}^{\text{H}}$ and $\mathbf{A}^{\text{H}}\mathbf{A}$ share the same rank and the first L eigenvalues, we use the condition number of matrix $\mathbf{A}^{\text{H}}\mathbf{A}$. Due to the invariance of the matrix trace, the condition number mainly reflects the smallest SS eigenvalue in a normalized sense.

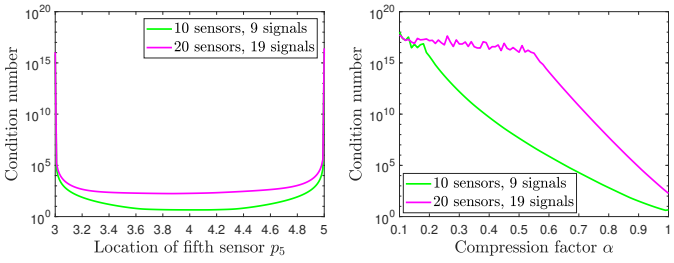

(a) Shifting sensor position p_5 (b) Compressing the ULA

Fig. 1: Variation of the condition number of $\mathbf{A}^{\text{H}}\mathbf{A}$ in two scenarios.

In the following two subsections, we numerically evaluate the variation of the condition number of matrix $\mathbf{A}^{\text{H}}\mathbf{A}$, by considering two baseline ULAs with $N_1 = 10$ and $N_2 = 20$ sensors, respectively, and the corresponding numbers of impinging signals in the two cases are respectively $L_1 = 9$ and $L_2 = 19$. In all cases, the signals are uniformly distributed in $[-60°, 60°]$. No noise is considered in this section.

4.1. Shifting a Single Sensor to an Off-Grid Position

We first examine the condition number of matrix $\mathbf{A}^{\text{H}}\mathbf{A}$ when the fifth sensor of each ULA at $p_5 = 4$ is shifted from its original position and moves closer to one of its neighboring sensors at $p_4 = 3$ and $p_6 = 5$. It is observed in Fig. 1(a) that, for each of the two scenarios, the condition number of the matrix $\mathbf{A}^{\text{H}}\mathbf{A}$ is minimum when the fifth sensor is located at its original position on the half-wavelength grid, i.e., p_5 = 4, representing that the smallest SS eigenvalue achieves the highest value. When the fifth sensor moves in either direction, the condition number increases, implying that the smallest SS eigenvalue becomes smaller. It is noticed that, for a higher number of array sensors, the condition number is higher but is less sensitive to the shift of the fifth sensor. In all array configurations, the condition number increases drastically when the position of the fifth sensor moves very close to either of the adjacent sensor positions at $p_4 = 3$ and $p_6 = 5$. In this case, the signal received at the fifth sensor is identical to the other sensor and, therefore, it no longer contributes to the array DOFs.

4.2. Compressing the Inter-Element Spacing of the ULA

Now we consider how the condition number of matrix $\mathbf{A}^{\text{H}}\mathbf{A}$ varies as the inter-element spacing of the two ULAs is compressed by a factor of α with α varying between 0.1 and 1. From Fig. 1(b) it can be observed that the condition number is minimum when $\alpha = 1$, i.e., the original ULAs with half-wavelength inter-element spacing, and increases monotonically as the compression factor decreases until the condition number saturates to a high value. This indicates that, as a ULA is compressed, the smallest eigenvalue reduces. It is observed that, as the value of α reduces, the condition number increases at a much faster rate for a ULA with a higher number of sensors. In other words, the smallest SS eigenvalues is more sensitive to the array inter-element compression for a larger ULA.

5. DOA ESTIMATION PERFORMANCE

In this section, we use the MUSIC algorithm to evaluate the DOA estimation performance for the two scenarios considered in the previous section, namely, when the array sensors are either shifted or

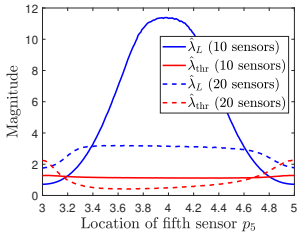

(a) Magnitude of $\hat{\lambda}_L$ and $\hat{\lambda}_{\text{thr}}$ with varying sensor locations of p_5.

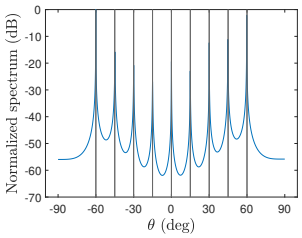

(b) All $L = 9$ sources are detected when $N = 10$ and $p_5 = 4.5$.

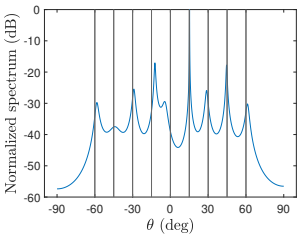

(c) All $L = 9$ sources not detected when $N = 10$ and $p_5 = 4.87$.

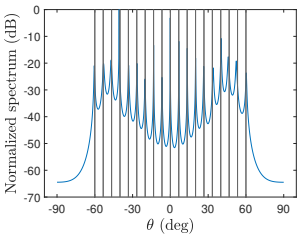

(d) All $L = 19$ sources detected when $N = 20$ and $p_5 = 4.87$.

Fig. 2: Eigenvalues and MUSIC spectra when shifting sensor position p_5.

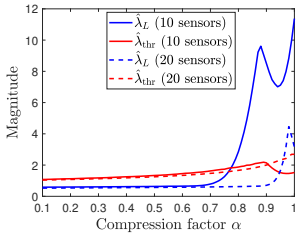

(a) Magnitude of $\hat{\lambda}_L$ and $\hat{\lambda}_{\text{thr}}$ with varying compression factor α.

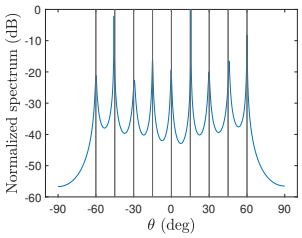

(b) All $L = 9$ sources detected when $N = 10$ and $\alpha = 0.85$.

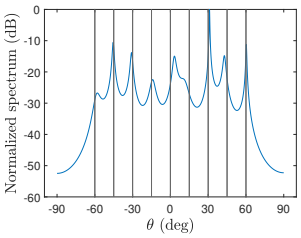

(c) All $L = 9$ sources not detected when $N = 10$ and $\alpha = 0.7$.

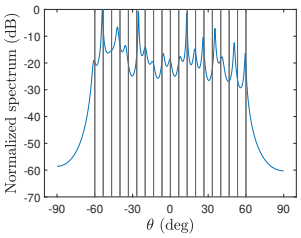

(d) All $L = 19$ sources not detected when $N = 20$ and $\alpha = 0.85$.

Fig. 3: Eigenvalues and MUSIC spectra when compressing the ULA.

compressed. We consider two ULAs consisting of $N_1 = 10$ and $N_2 = 20$ sensors, respectively with $L_1 = 9$ and $L_2 = 19$ uncorrelated signals uniformly distributed in $[-60°, 60°]$. 1,000 snapshots are assumed and the input signal-to-noise ratio (SNR) is set to 5 dB.

5.1. Shifting a Single Sensor to an Off-Grid Position

For the first scenario in which we consider that only a single sensor is shifted from its integer location to a non-integer one, we shift the fifth sensor, originally located at $p_5 = 4$, to all fractional locations on either side between $p_5 = 3$ and $p_5 = 5$. Fig. 2(a) shows how the estimated smallest SS eigenvalue $\hat{\lambda}_L$ and the QR factorization threshold $\hat{\lambda}_{\text{thr}} = ||\mathbf{R}_{22}||_2$ change for the two ULAs as p_5 is varied. It is observed that, when $p_5 < 3.19$ and $p_5 > 4.80$, λ_L for the 10-element ULA falls below the threshold, i.e., $\lambda_L \leq \lambda_{\text{thr}}$ and, correspondingly, the numerical rank of $\hat{\mathbf{R}}_x$ representing the number of identifiable signals of the array drops from 9 to 8. In Fig. 2(b), we show that, when $p_5 = 4.5$, all the $L = 9$ signals are clearly resolved using the MUSIC algorithm. On the other hand, when $p_5 = 4.87$, as shown in the MUSIC spectrum depicted in Fig. 2(c), the signals are not clearly resolved.

To compare the performance between arrays with a different number of sensors, as discussed in Fig. 1(a), with an increasing number of array sensors in the ULA, the condition number becomes less sensitive to the position change. Fig. 2(a) verifies that, for the 20-sensor array case, the crossing point of the estimated smallest SS eigenvalue $\hat{\lambda}_L$ and the RQ factorization threshold $\hat{\lambda}_{\text{thr}}$ moves closer to the two edges and becomes 3.07 and 4.90, respectively. Compared to the 10-sensor array, the 20-sensor array has a wider range of non-integer positions to which the fifth sensor can be shifted without losing a DOF. Correspondingly, when the 20-element array with 19 impinging signals is considered, it is observed in Fig. 2(d) that all sources are still resolved via MUSIC when $p_5 = 4.87$, thus validating our claims.

5.2. Compressing the Inter-Element Spacing of the ULA

Fig. 3(a) shows the variation of the estimated smallest SS eigenvalue $\hat{\lambda}_L$ and the QR factorization threshold $\hat{\lambda}_{\text{thr}}$ with respect to the compression factor α for both 10- and 20-element arrays. It can be seen that the smallest SS eigenvalue λ_L is above the threshold λ_{thr} when $\alpha > 0.78$ for the 10-element array and $\alpha > 0.96$ for the 20-element array. These results are consistent with the observations made in Fig. 1(b) that an array with a higher number of sensors is more sensitive to the compression factor α.

Fig. 3(b) shows the estimated MUSIC spatial spectrum of the 10-element array which indicates that all the $L = 9$ signals are detected when the compression factor is $\alpha = 0.85$. As the compression factor is further reduced to $\alpha = 0.75$, as shown in Fig. 3(c), the 10-element array fails to correctly identify the 9 signals. On the other hand, as the 20-element array is more sensitive to the inter-element compression, it is observed in Fig. 3(d) that it cannot resolve all 19 sources even when α is 0.85.

6. CONCLUSION

In this paper, we examined the effect of placing array sensors off the half-wavelength grid on the number of achievable DOFs of the array. We analyzed the smallest SS eigenvalue in relation to the change in sensor positions and gain insights into how the sensors can be placed in non-integer positions without losing the DOFs. Such analysis is achieved by exploiting the rank-revealing QR factorization, and the signal identifiability is represented in terms of the numerical rank of the covariance matrix. Such analyses gave us insights in the design of sparse array configurations, particularly in the context of rational sparse arrays.

7. REFERENCES

[1] H. L. Van Trees, *Optimum Array Processing: Part IV of Detection, Estimation, and Modulation Theory*. Wiley, 2002.

[2] T. E. Tuncer and B. Friedlander (Eds.), *Classical and Modern Direction-of-Arrival Estimation*, Academic Press, 2009.

[3] P. Pal and P. P. Vaidyanathan, "Nested arrays: A novel approach to array processing with enhanced degrees of freedom," *IEEE Trans. Signal Process.*, vol. 58, no. 8, pp. 4167–4181, Aug. 2010.

[4] P. P. Vaidyanathan and P. Pal, "Sparse sensing with co-prime samplers and arrays," *IEEE Trans. Signal Process.*, vol. 59, no. 2, pp. 573–586, Feb. 2011.

[5] S. Qin, Y. D. Zhang, and M. G. Amin, "Generalized coprime array configurations for direction-of-arrival estimation," *IEEE Trans. Signal Process.*, vol. 63, no. 6, pp. 1377–1390, March 2015.

[6] J. Liu, Y. Zhang, Y. Lu, S. Ren, and S. Cao, "Augmented nested arrays with enhanced DOF and reduced mutual coupling," *IEEE Trans. Signal Process.*, vol. 65, no. 21, pp. 5549–5563, Nov. 2017.

[7] Z. Zheng, W. Wang, Y. Kong and Y. D. Zhang, "MISC Array: A new sparse array design achieving increased degrees of freedom and reduced mutual coupling effect," *IEEE Trans. Signal Process.*, vol. 67, no. 7, pp. 1728–1741, April 2019.

[8] W. Shi, Y. Li, and R. C. de Lamare. "Novel sparse array design based on the maximum inter-element spacing criterion," *IEEE Signal Process. Lett.*, vol. 29, pp. 1754–1758, July 2022.

[9] S. Wandale and K. Ichige, "Flexible extended nested arrays for DOA estimation: Degrees of freedom perspective," *Signal Process.*, vol. 201, no. 108710, pp. 1–10, Dec. 2022.

[10] A. Ahmed and Y. D. Zhang, "Generalized non-redundant sparse array designs," *IEEE Trans. Signal Process.*, vol. 69, pp. 4580–4594, Aug. 2021.

[11] A. Moffet, "Minimum-redundancy linear arrays," *IEEE Trans. Antennas Propagat.*, vol. 16, no. 2, pp. 172–175, March 1968.

[12] R. T. Hoctor and S. A. Kassam, "The unifying role of the coarray in aperture synthesis for coherent and incoherent imaging," *Proc. IEEE*, vol. 78, no. 4, pp. 735–752, April 1990.

[13] Q. Shen, W. Liu, W. Cui, S. Wu, Y. D. Zhang, and M. G. Amin, "Low-complexity wideband direction-of-arrival estimation based on co-prime arrays," *IEEE/ACM Trans. Audio, Speech and Language Process.*, vol. 23, no. 9, pp. 1445–1456, Sept. 2015.

[14] S. Qin, Y. D. Zhang, M. G. Amin, and B. Himed, "DOA estimation exploiting a uniform linear array with multiple coprime frequencies," *Signal Process.*, vol. 130, pp. 37–46, Jan. 2017.

[15] A. Liu, X. Zhang, Q. Yang, and W. Deng, "Fast DOA estimation algorithms for sparse uniform linear array with multiple integer frequencies," *IEEE Access*, vol. 6, pp. 29952–29965, 2018.

[16] S. Zhang, A. Ahmed, Y. D. Zhang, and S. Sun, "Enhanced DOA estimation exploiting multi-frequency sparse array," *IEEE Trans. Signal Process.*, vol. 69, pp. 5935–5946, Oct. 2021.

[17] G. Qin, M. G. Amin, and Y. D. Zhang, "DOA estimation exploiting sparse array motions," *IEEE Trans. Signal Process.*, vol. 67, no. 11, pp. 3013–3027, June 2019.

[18] H. Wu, Q. Shen, W. Cui, and W. Liu, "DOA estimation with nonuniform moving sampling scheme based on a moving platform," *IEEE Signal Process. Lett.*, vol. 28, pp. 1714–1718, 2021.

[19] P. J. Bevelacqua and C. A. Balanis, "Optimizing antenna array geometry for interference suppression," *IEEE Trans. Antennas Propagat.*, vol. 55, no. 3, pp. 637-641, March 2007.

[20] M. Rubsamen and A. B. Gershman, "Direction-of-arrival estimation for nonuniform sensor arrays: From manifold separation to Fourier domain MUSIC methods," *IEEE Trans. Signal Process.*, vol. 57, no. 2, pp. 588–599, Feb. 2009.

[21] Y. I. Abramovich, N. K. Spencer and A. Y. Gorokhov, "DOA estimation for noninteger linear antenna arrays with more uncorrelated sources than sensors," *IEEE Trans. Signal Process.*, vol. 48, no. 4, pp. 943-955, April 2000.

[22] P. Kulkarni and P. P. Vaidyanathan, "Non-integer arrays for array signal processing," *IEEE Trans. Signal Process.*, vol. 70, pp. 5457–5472, 2022.

[23] P. Kulkarni and P. P. Vaidyanathan, "Rational arrays for DOA estimation," in *Proc. IEEE Int. Conf. Acoust., Speech, Signal Process. (ICASSP)* , Singapore, 2022, pp. 5008–5012.

[24] M. Wagner, Y. Park, and P. Gerstoft, "Gridless DOA estimation and root-MUSIC for non-uniform linear arrays," *IEEE Trans. Signal Process.*, vol. 69, pp. 2144-2157, 2021.

[25] Y. D. Zhang and M. G. Amin, "Multi-frequency rational sparse array for direction-of-arrival estimation," in *Proc. Int. Symp. Signals, Circuits and Systems*, Iași, Romania, July 2023.

[26] M. W. T. S. Chowdhury and Y. D. Zhang, "Unambiguous DOA estimation using multi-frequency rational sparse arrays," in *Proc. Asilomar Conf. Signals, Syst. Comput.*, Pacific Grove, CA, Oct. 2023.

[27] V. T. Ermolaev and A. B. Gershman, "Fast algorithm for minimum-norm direction-of-arrival estimation," *IEEE Trans. Signal Process.*, vol. 42, no. 9, pp. 2389-2394, Sept. 1994.

[28] S. Ubaru, Y. Saad, and A. Seghouane, "Fast estimation of approximate matrix ranks using spectral densities," *Neural Comput.*, vol. 29, no. 5, pp. 1317–1351, May 2017.

[29] Y. P. Hong, and C.T. Pan, "Rank-revealing QR factorizations and the singular value decomposition," *Math. Comput.*, vol. 58, no. 197, 1992, pp. 213–32.

[30] T. F. Chan and P. C. Hansen, "Some applications of the rank revealing QR factorization," *SIAM J. Scientific Stat. Comput.*, vol. 13, pp. 727–741, 1992.

[31] M. Gu and S. C. Eisenstat, "Efficient algorithms for computing a strong rank revealing QR factorization," *SIAM J. Scientific Comput.*, vol. 17, pp. 848–869, 1996.

[32] J. A. Ball, I. Gohberg, L. Rodman, and T. Shalom, "On the eigenvalues of matrices with given upper triangular part," *Integral Equ. Oper. Theory*, vol. 13, pp. 488–497, 1990.

[33] W. H. Haemers, "Interlacing eigenvalues and graphs," *Linear Algebra App.*, vol. 226, pp. 593–616, 1995.

[34] X. Chen, and S. N. Zheng, "A unified proof of interlacing properties of eigenvalues of totally positive matrices," *Linear Algebra App.*, vol. 632, pp. 241–245, Jan. 2022.